



Muhammad A. Ali  
Rehan Umer  
Kamran A. Khan

# CT Scan Generated Material Twins for Composites Manufacturing in Industry 4.0

# CT Scan Generated Material Twins for Composites Manufacturing in Industry 4.0

Muhammad A. Ali · Rehan Umer ·  
Kamran A. Khan

# CT Scan Generated Material Twins for Composites Manufacturing in Industry 4.0

 Springer

Muhammad A. Ali  
Department of Aerospace Engineering  
Khalifa University of Science  
and Technology  
Abu Dhabi, United Arab Emirates

Rehan Umer  
Department of Aerospace Engineering  
Khalifa University of Science  
and Technology  
Abu Dhabi, United Arab Emirates

Kamran A. Khan  
Department of Aerospace Engineering  
Khalifa University of Science  
and Technology  
Abu Dhabi, United Arab Emirates

ISBN 978-981-15-8020-8

ISBN 978-981-15-8021-5 (eBook)

<https://doi.org/10.1007/978-981-15-8021-5>

© The Editor(s) (if applicable) and The Author(s), under exclusive license to Springer Nature Singapore Pte Ltd. 2020

This work is subject to copyright. All rights are solely and exclusively licensed by the Publisher, whether the whole or part of the material is concerned, specifically the rights of translation, reprinting, reuse of illustrations, recitation, broadcasting, reproduction on microfilms or in any other physical way, and transmission or information storage and retrieval, electronic adaptation, computer software, or by similar or dissimilar methodology now known or hereafter developed.

The use of general descriptive names, registered names, trademarks, service marks, etc. in this publication does not imply, even in the absence of a specific statement, that such names are exempt from the relevant protective laws and regulations and therefore free for general use.

The publisher, the authors and the editors are safe to assume that the advice and information in this book are believed to be true and accurate at the date of publication. Neither the publisher nor the authors or the editors give a warranty, expressed or implied, with respect to the material contained herein or for any errors or omissions that may have been made. The publisher remains neutral with regard to jurisdictional claims in published maps and institutional affiliations.

This Springer imprint is published by the registered company Springer Nature Singapore Pte Ltd. The registered company address is: 152 Beach Road, #21-01/04 Gateway East, Singapore 189721, Singapore

# Acknowledgements

This book is based on research conducted at Khalifa University of Science and Technology (KUST), Abu Dhabi, United Arab Emirates. We are thankful to KUST for providing funding for conducting this research. We are thankful to Prof. Wesley J. Cantwell, Director Aerospace Research and Innovation Center (ARIC), for his valuable guidance throughout this work. We also appreciate the efforts of the research and support staff at KUST, Mr. Pradeep George, Mr. Jimmy Thomas, and Dr. Alia Aziz, for their involvement at various stages of this research. We are eternally indebted to our families for their unconditional support throughout the project. We are also profoundly grateful to fellow researchers, Dr. Yarjan Abdul Samad, Dr. Waqas Waheed, Dr. Adnan Saeed, Dr. Nguyen V. Viet, and Dr. Shaohong Luo.

Finally, we would like to thank the publishing team at Springer Nature Scientific who tirelessly worked to put all the bits together. A special thanks to the project coordinator books production, Mr. Sriram Srinivas, for guiding us throughout the publication process.

Muhammad A. Ali  
Rehan Umer  
Kamran A. Khan

# Contents

<b>1</b>	<b>Introduction</b>	1
1.1	Background	1
1.2	Manufacturing of Fiber Reinforced Polymer Composites	2
1.2.1	Liquid Composite Molding	3
1.3	Reinforcement Characterization	4
1.3.1	Reinforcement Compaction Response	5
1.3.2	Reinforcement Permeability	6
1.4	State-of-the-Art	7
1.4.1	Compaction Characterization	7
1.4.2	Permeability Characterization	9
1.4.3	Material Twin Based Characterization Framework	14
1.5	Motivation and Objectives	15
1.6	Book Outline	16
	References	16
<b>2</b>	<b>Generation of Material Twin Using Micro CT Scanning</b>	19
2.1	XCT Setup	20
2.1.1	Compaction Setup	20
2.1.2	XCT Machine	21
2.1.3	Fabric Samples	22
2.1.4	Noise Reducing Filters	22
2.1.5	Radiographic Projections	23
2.2	Data Processing	24
2.2.1	3D Volume Reconstruction	25
2.2.2	Segmentation	26
2.3	Tow Deformations and Compaction Response	30
2.4	Model Generation	36
2.4.1	Material Twin	36
2.4.2	Stochastic Virtual Model	38
2.4.3	Simplified Models	40

2.5	Virtual Permeability	42
2.5.1	Numerical Setup	42
2.6	Summary	45
	References	46
<b>3</b>	<b>Experimental Techniques for Reinforcement Characterization</b>	<b>53</b>
3.1	Types of Reinforcements	54
3.1.1	3D Reinforcements	54
3.1.2	2D Reinforcements	55
3.1.3	AFP Carbon Tape	56
3.2	Test Fluid	57
3.3	Sample Preparation	57
3.4	Compaction Tests	59
3.5	Permeability Measurement	60
3.5.1	Through-Thickness Permeability Measurement	60
3.5.2	In-Plane Permeability Measurement	62
3.6	Discussions	66
3.6.1	Compaction Tests	66
3.6.2	Through-Thickness Permeability Measurements	67
3.6.3	In-Plane Permeability Measurements	69
3.7	Summary	70
	References	71
<b>4</b>	<b>Experimental-Numerical Hybrid Reinforcement Characterization Framework</b>	<b>73</b>
4.1	Overview	73
4.2	The In Situ Computed Tomography System	75
4.2.1	Micro CT Equipment	75
4.2.2	In Situ Compression Fixture	75
4.2.3	Data Acquisition	76
4.2.4	Load and Displacement Control	76
4.2.5	3D Visualization	77
4.3	Micro CT Data Acquisition	78
4.3.1	Sample Preparation	78
4.3.2	Scan Settings	79
4.3.3	Setting the Scan Resolution	79
4.4	Data Processing and Digital Experiments	80
4.4.1	Data Pre-processing and Segmentation	80
4.4.2	Digital Flow Experiments	80
4.4.3	Pore Structure Analysis	82
4.5	Generation of Digital Material Twins	83
4.5.1	Realistic Voxel Model	83
4.5.2	Stochastic Virtual Model of the AFP Carbon Tape	87
4.5.3	Ideal Model	89

- 4.6 Flow Modeling . . . . . 90
  - 4.6.1 Micro-Scale Flow Modeling . . . . . 90
  - 4.6.2 Meso-Scale Flow Modeling . . . . . 91
- 4.7 Flow and Boundary Conditions . . . . . 92
- 4.8 Permeability Computation . . . . . 92
- 4.9 Summary . . . . . 93
- References . . . . . 93
- 5 Reinforcement Compaction Response . . . . . 95**
  - 5.1 Stress Relaxation . . . . . 95
    - 5.1.1 Multi-stage Compaction . . . . . 95
    - 5.1.2 Multi-cycle Compaction . . . . . 97
  - 5.2 Tow Deformations . . . . . 97
    - 5.2.1 3D Orthogonal Reinforcement . . . . . 98
    - 5.2.2 3D Angle Inter-lock Reinforcement . . . . . 99
  - 5.3 Gap Analysis of the 3D Reinforcements . . . . . 101
    - 5.3.1 Gap Analysis of 3D Orthogonal Reinforcement . . . . . 101
    - 5.3.2 Gap Analysis of Angle Inter-lock Reinforcement . . . . . 105
  - 5.4 Pore Network Analysis of the Angle Inter-lock Reinforcement . . . . . 105
    - 5.4.1 Pore Size Distribution . . . . . 106
    - 5.4.2 Path Analysis . . . . . 106
    - 5.4.3 Effect of Multi-cycle Compaction on the Pore Size Distribution . . . . . 108
  - 5.5 Application of the Hybrid Characterization Framework to AFP Carbon Tape . . . . . 108
    - 5.5.1 Stress Relaxation . . . . . 109
    - 5.5.2 Microscopic Analysis . . . . . 109
    - 5.5.3 Gap Analysis . . . . . 110
  - 5.6 Summary . . . . . 111
  - References . . . . . 113
- 6 Flow Fields and Reinforcement Permeability . . . . . 115**
  - 6.1 Through-Thickness Permeability of the 3D Reinforcements . . . . . 115
    - 6.1.1 Velocity Fields in Through-Thickness Flow . . . . . 116
    - 6.1.2 Through-Thickness Permeability Predictions . . . . . 118
  - 6.2 In-Plane Permeability of the 3D Reinforcements . . . . . 120
    - 6.2.1 Velocity Fields in In-Plane Flow . . . . . 120
    - 6.2.2 In-Plane Permeability Predictions . . . . . 123
  - 6.3 Analysis of Variability in Permeability Predictions . . . . . 126
    - 6.3.1 Variability Among Unit Cells . . . . . 127
    - 6.3.2 Variability Within Unit Cells . . . . . 129
  - 6.4 Effect of Unit Cell Size on Permeability Predictions . . . . . 129
  - 6.5 Kozeny-Carman Analysis . . . . . 131



6.6	Effect of Cyclic Compaction on Permeability . . . . .	133
6.6.1	Velocity Fields . . . . .	135
6.6.2	Virtual Permeability Predictions . . . . .	135
6.7	Application of the Hybrid Characterization Framework to Other Reinforcements. . . . .	139
6.7.1	Through-Thickness Permeability of AFP Carbon Tape . . . . .	139
6.7.2	In-Plane Permeability of AFP Carbon Tape . . . . .	142
6.7.3	2D Benchmark Reinforcements . . . . .	144
6.8	Summary . . . . .	150
	References . . . . .	151
<b>7</b>	<b>Experimental-Empirical Hybrid Approach . . . . .</b>	<b>153</b>
7.1	Basic Formulation . . . . .	154
7.1.1	Porous Regions in Parallel . . . . .	154
7.1.2	Porous Regions in Series . . . . .	155
7.2	Breakdown of 3D Architecture . . . . .	157
7.3	In-Plane Permeability of the 3D Architecture . . . . .	157
7.3.1	Permeability of the Channel and Gap . . . . .	160
7.3.2	Equivalent Permeability of the Channel-Warp Combination . . . . .	161
7.3.3	Equivalent Permeability of the Gap-Binder Combination . . . . .	161
7.3.4	Equivalent Permeability of the Region A and C . . . . .	162
7.3.5	Equivalent Permeability of the Channel-Gap-Binder Combination . . . . .	162
7.3.6	Equivalent Permeability of the Warp-Channel-Gap- Binder Combination . . . . .	162
7.3.7	Equivalent Permeability of Region B . . . . .	163
7.3.8	Overall Permeability . . . . .	163
7.4	Through-Thickness Permeability of the 3D Architecture . . . . .	163
7.5	Numerical Validation . . . . .	164
7.5.1	Modeling Approach . . . . .	164
7.5.2	Validation of Basic Formulation . . . . .	165
7.5.3	Validation of Permeability Models for the 3D Architecture. . . . .	167
7.6	Summary . . . . .	169
	References . . . . .	169

# Chapter 1

## Introduction



### 1.1 Background

The availability of adequate materials has been a significant factor in the advancement of human civilization and technological breakthroughs. Throughout the ages, the constant improvements in the mechanical, electrical and thermal properties of materials have been pushing the limits of technology. In these advancements, composite materials represent a giant leap with promising characteristics for high performance, lightweight and multifunctional applications. The design and manufacturing of composite materials and structures has been pursued in evolutionary as well as revolutionary ways during the past few decades [1]. Constant progress is being made in the development of existing techniques through research and experiments, as well as new ideas that are being presented. These efforts aim at reducing the manufacturing cost and complexity, enhancing the quality of parts produced and minimizing environmental impacts.

A composite material is a material made from two or more constituent materials with significantly different physical or chemical properties that, when combined, produce a material with characteristics different from the individual components. The individual components remain separate and distinct within the final part. Fiber Reinforced Polymer Composite (FRPC) is a class of composite materials that consists of a polymer matrix reinforced with high-strength natural or synthetic fibers. The reinforcing fiber adds rigidity and is the main load-bearing component of the composite materials. While high performance composites are dominated by synthetic glass, carbon and aramid fibers, a wide range of natural fibers is also gaining popularity. The matrix binds the fibers together, transmits applied loads to the fibers, prevents propagation of cracks and protects the fibers from damage. Polymer matrices are classified as thermoplastic or thermosetting resins. A thermosetting polymer is irreversibly cured from a soft solid or viscous liquid, whereas a thermoplastic polymer becomes pliable or moldable above a specific temperature and solidifies upon cooling.

The advantages of FRPC over other materials have attracted many industries such as aerospace, automobile, infrastructure, sports and marine to explore and increase their usage. FRPC materials have been used extensively in a wide variety of aerospace applications, ranging from commercial airliners to deep space vehicles. World-leading organizations in aerospace such as National Aeronautics and Space Administration (NASA), the European Space Agency (ESA), Boeing, Airbus, Bombardier etc. are investing intensively in developing such materials. The commercial airliners, the Boeing 787 and the Airbus A350 are excellent examples, where more than 50% of the structure is comprised of fiber reinforced composites. NASA recently achieved a major milestone in the advancement of space technology by successfully testing a pressurized, large cryogenic propellant tank made entirely out of fiber reinforced composite materials. In automobile manufacturing, FRPC materials offer major advantages over steel and similar metals in producing lighter, safer and more fuel-efficient vehicles. FRPC materials are now being used in automobile body, chassis, interiors and engine components. Recently, several high value vehicles, such as the BMW M, and the i-series have used carbon fiber reinforced composites as primary structures. Apart from these two major industries, fiber reinforced composites have been the focus of many other industries, such as marine, defense, sports and energy sectors. For example, entire wind turbine blades are being manufactured using advanced composite manufacturing techniques. Sport items such as, tennis rackets, snow skis, sail boats, kayaks, helmets, shoe soles, hockey sticks, etc. are also being manufactured from fiber reinforced polymer composites.

## 1.2 Manufacturing of Fiber Reinforced Polymer Composites

Fiber reinforcements are typically in the form of random mats, woven reinforcements, unidirectional or non-crimp stitched reinforcements, knits, braids, or 3D woven reinforcements [2]. Such types of reinforcement are developed into composite parts through various composite manufacturing techniques. The quality of the composite material and the resulting part depends on the manufacturing process, since it is during the manufacturing process that the matrix material and the fiber reinforcement are combined and consolidated to form the composite part. The process depends on the type of resin and reinforcement used. In this book, the focus is mainly on composites manufacturing process characterization which can be used in autoclave and Out-of-Autoclave (OoA) manufacturing techniques. In the autoclave process, the fiber reinforcements are used in the form of prepregs. The prepregs are cut and formed into the desired shape and placed on a rigid mold in the desired position, orientation and sequence to form a layup. The layup, sealed with vacuum bag, is then placed into the autoclave and the curing process is performed according to the prescribed temperature-pressure-vacuum-time cycle inside the autoclave. The process is very versatile and gives a very uniform quality, as pressure and heat can be regulated

very precisely. On the other hand, it is very costly due to high capital cost and time consuming due to long layup and curing time. The Out-of-Autoclave manufacturing includes processes such as vacuum bag only (VBO) and liquid composite molding (LCM). The main advantage of OoA processing techniques is the low capital cost. LCM techniques are attractive as they provide excellent control over part thickness hence, excellent mechanical properties are possible. However, the process characterization and quality control tools are still under development and require considerable research to achieve repeatable part quality. This book will focus on new LCM reinforcement characterizations (compaction response and permeability) techniques based on micro CT imaging.

### 1.2.1 Liquid Composite Molding

Liquid composite molding (LCM) processes involve impregnation of a reinforcement using a liquid resin with “injectable” viscosity. A generic LCM process utilizes a mold cavity that is in the shape of the part to be manufactured. The fiber reinforcement is placed inside the mold cavity and the mold is closed. A reactive (thermoset) resin is then injected into the mold cavity under pressure, until complete saturation of the reinforcing material is achieved. The resin is then allowed to cure, after curing, the part is de-molded to yield the finished product. These steps are illustrated in Fig. 1.1.

Liquid composite molding process has several variants with minor differences. Some of these variants of LCM processes are shown in Fig. 1.2. Resin Transfer

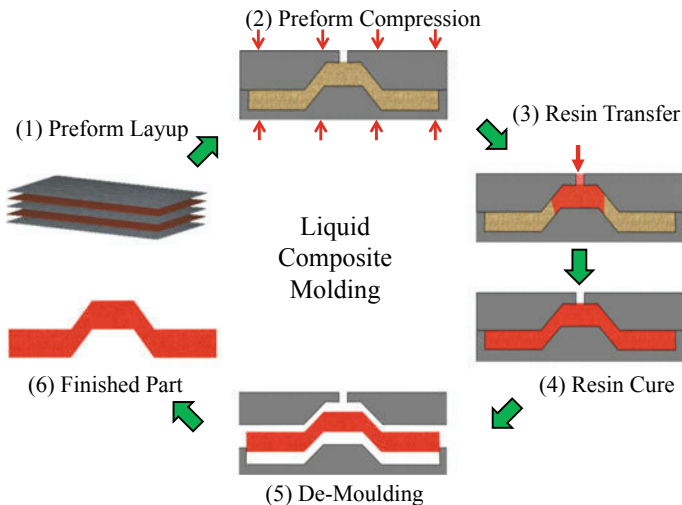
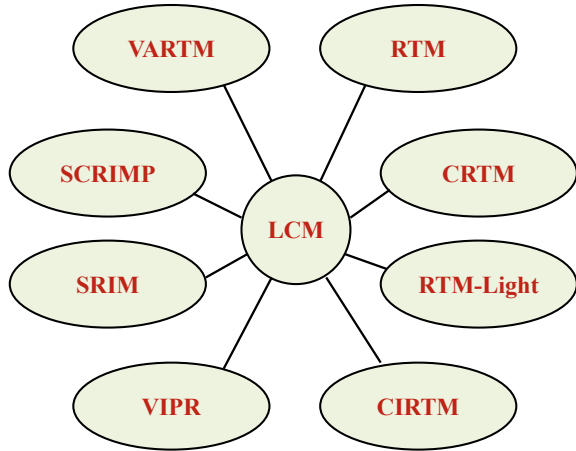


**Fig. 1.1** Schematic illustration of various steps involved in manufacturing of composite parts using liquid composite molding process

**Fig. 1.2** Various variations of liquid composite molding technique



Molding (RTM) and Compression Resin Transfer Molding (CRTM) employ two rigid molds that enable a high compaction force to be applied with minimal mold deflections. RTM-light uses semi-flexible plastic or composite molds, providing a medium level compaction while minimizing mold deflections at a much reduced cost.

The Vacuum Assisted Resin Transfer Molding (VARTM) and Seemann's Composite Resin Infusion Molding Process (SCRIMP) are slight modifications of the process where the top half of the mold is replaced by a vacuum bag. In SCRIMP, a highly permeable layer is introduced at the top or the bottom of the reinforcement to facilitate rapid distribution of the resin throughout the part. Both VARTM and SCRIMP rely on drawing the resin from a container at atmospheric pressure through the fibrous bed by creating a vacuum. These processes have replaced RTM for many applications due to their simplicity, low initial capital investment and the ability to manufacture large structures. The cost is low due to low pressures used in the manufacturing process and the curing reactions being carried out mostly at room temperature. The process requires only a single tool surface, while the top surface is covered with a vacuum bag which also cuts down on tooling costs. The disadvantages of VARTM process is rough surface finish on the bag side, the time required in material preparation, inconsistent dimensional tolerances and the lack of automation.

### 1.3 Reinforcement Characterization

During the LCM process, reinforcement compaction inside the mold cavity and successful injection of the resin plays an important role to ensure part quality. These two steps are primarily dependent on the reinforcement compressibility and permeability. Hence, for better process optimization and modeling, the compaction

response and permeability of the reinforcement need to be determined. These two characteristics are considered vital processing parameters in LCM.

### ***1.3.1 Reinforcement Compaction Response***

In an LCM process, once a dry fiber reinforcement is placed inside the mold cavity, the mold is closed using either a hydraulic press or vacuum bag. The behavior of a reinforcement subjected to an applied force normal to its plane has important consequences on the mold design and equipment specifications for all processes using fiber reinforcements. For example, in VARTM, the clamping force is applied using vacuum pressure under a flexible tooling, while in the RTM process, the reinforcement is compacted between two rigid molds. In either case, the reinforcement compaction response influences the mold clamping force, part thickness and fiber volume fraction, as a result, affecting the reinforcement permeability. The compaction step is vital since, prior to manufacture, the fibrous material is not yet at the desired fiber volume fraction. The compaction decreases reinforcement thickness and increases fiber volume fraction. Furthermore, in some cases, the reinforcements are intentionally subjected to transverse compaction in order to “de-bulk” to a high fiber volume fraction [3]. The reinforcements can be subjected to single-cycle, multi-cycle or multi-stage compaction [4]. Moreover, during the resin injection, the reinforcement is not only subjected to the mold clamping force provided by the press, but also to the fluid pressure generated as a result of resin injection. The total stress acting on the reinforcement is governed by Terzaghi’s law which states that the total stress carried by the reinforcement is equal to the sum of the compaction stress taken by the fibers and fluid pressure [5–8]. Due to the compaction stress, the internal architecture of the reinforcement also changes, i.e. the tows flatten, the spaces between the fiber tows decrease, the tows undergo bending while at the micro-scale, the gaps between individual fibers also decrease. The compaction of multiple layered reinforcements (a stack of a number of 2D textiles) possess additional complexity of nesting, inter-layering and packing. Hence, during manufacturing of composite parts via LCM process, the transverse compaction is important and it is essential to characterize the compaction response of the reinforcing fabric.

In any reinforcement compaction characterization, two major attributes need to be investigated; (1) the relationship between applied load and the resulting thickness or fiber volume fraction ( $V_f$ ) and, (2) microscopic geometrical changes of the tows and fibers. The relationship between applied stress and/or resulting thickness (fiber volume fraction) is presented as a stress relaxation curve. The standard stress relaxation curve is a plot of applied stress versus time or fiber volume fraction ( $V_f$ ). Typically, the compaction of reinforcement consists of two parts, i.e. dynamic, non-linear compression stage and stress relaxation. The compaction depends on the reinforcement architecture, speed, dry/wet state, and number of reinforcement layers used. The second objective of a compaction study is to document tow deformations and

the inter-tow gap reduction as a result of decreasing thickness, this is achieved by microscopic investigation either in-situ or ex-situ.

### 1.3.2 Reinforcement Permeability

In the LCM process, the impregnation of reinforcement with resin is considered as flow through porous medium phenomena, and the permeability of the reinforcement dictates the “ease” of advancement of the resin flow front through the open channels therefore, influencing mold filling time. As the Reynolds number of the resin flow is considered very low due to low flow velocities, the resin flow through the reinforcement is assumed to be governed by Darcy’s law. The Darcy’s law relates the volume flow rate of a Newtonian fluid through a porous media of given cross-sectional area and the pressure gradient along the flow direction. The parameters included in Darcy’s law are illustrated in Fig. 1.3a. Mathematically, Darcy’s law is given as,

$$Q = -K \frac{A}{\mu} \frac{P_i - P_o}{L} = -K \frac{A \Delta P}{\mu L} \quad (1.1)$$

where  $Q$  is the volume flow rate of the fluid,  $K$  is the permeability tensor,  $\mu$  is the dynamic fluid viscosity,  $P_i - P_o$  is the pressure gradient or the pressure difference,  $A$  is the cross-sectional area, and  $L$  is the length of the medium across which the fluid flows. The permeability is a measure of the ability of a porous material to allow fluid to pass through it and is also related to its porous structure and the connectivity of the pores. The Permeability is a directional quantity, described by a tensor in three dimensions. The 3D permeability tensor  $K$  can be expressed in Cartesian coordinates as,

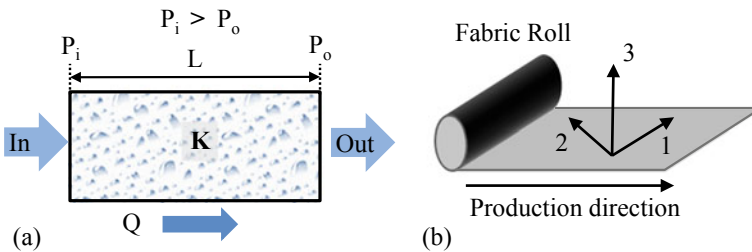


**Fig. 1.3** Illustration of **a** flow through a porous medium with relevant parameters and **b** principle permeability directions for a typical reinforcement

$$\mathbf{K} = \begin{bmatrix} K_{xx} & K_{xy} & K_{xz} \\ K_{yx} & K_{yy} & K_{yz} \\ K_{zy} & K_{zy} & K_{zz} \end{bmatrix} \quad (1.2)$$

In case of symmetry, the off-diagonal terms are usually taken equal. If the coordinate system is oriented in the principal directions, the off diagonal elements are taken as zero, and the remaining terms are known as principal permeability values i.e.  $K_{11}$ ,  $K_{22}$  and  $K_{33}$ . For fibrous reinforcement, they are divided as the in-plane,  $K_{11}$  and  $K_{22}$ , and through-thickness or transverse,  $K_{33}$ , permeabilities. The principal directions for a typical fibrous reinforcement are illustrated in Fig. 1.3b.

The reinforcement permeability is primarily a function of the reinforcement architecture and its fiber volume fraction ( $V_f$ ) [9]. Incorrect compaction and permeability predictions may lead to an inefficient process design through incorrect fiber volume fractions and mold filling time, dry spots and defects in the manufactured parts [3]. The permeability characterization of fiber reinforcements is important for liquid composite molding process modeling and simulations. The permeability dictates the time taken to fill the mold, the degree of fiber wetting by the resin and flow patterns generated as a result of resin flow.

## 1.4 State-of-the-Art

Existing reinforcement characterization techniques focus on compaction response and permeability characterization separately. A number of analytical, experimental and numerical methods exist for the prediction of both the compaction behavior and permeability of reinforcement as described below.

### 1.4.1 *Compaction Characterization*

#### 1.4.1.1 Theoretical Compaction Models

Available theoretical models for reinforcement compaction response relate the compaction stress to fiber volume fraction using an algebraic relationship. There are a number of such models which are derived from micro-, meso- or macro-scale compaction behavior. At the micro-scale, micro-mechanical models based on the elastic beam theory have been developed. Another commonly applied approach is the use of a semi-empirical model based on compaction characterization experiments. In this empirical approach, the compaction behavior is modelled using one or multiple non-linear elastic equations, or few more sophisticated models with parameters that are determined from experiments. The fibrous reinforcements have been found to have visco-elastic, plastic and visco-plastic behavior under compaction.



These efforts are mainly focused on developing models that account for inelastic reinforcement behavior.

#### 1.4.1.2 Experimental Compaction Characterization

The compaction response of fiber reinforcements can be obtained via performing compaction experiments on a universal testing machine equipped with a load cell and displacement measuring sensors. Generic experimental procedures involve; compressing test sample between two flat and rigid platens installed in a universal testing machine. A typical setup of a reinforcement compaction test is shown in Fig. 1.4. The rate of compression, as well as the target load or thickness is controlled via integrated software. The applied load and the displacement of the platens are also recorded. The data is converted into stress versus time or fiber volume fraction curve. The cavity thickness and  $V_f$  are related by the following equation,

$$V_f = \frac{A_w N}{\rho_s h} \quad (1.3)$$

where  $A_w$  is the areal weight of the reinforcement,  $N$  is the number of layers,  $\rho_s$  is the density of fiber and  $h$  is the cavity thickness.

In order to investigate the internal deformations, composite parts are manufactured using the separate test sample, to which the compaction levels of interest are applied. The part is then cut such that its cross-section may be viewed using an optical microscope or a Scanning Electron Microscope [SEM]. However, this step is independent of the compaction test and requires fresh test samples, as well as a very different set of equipment.

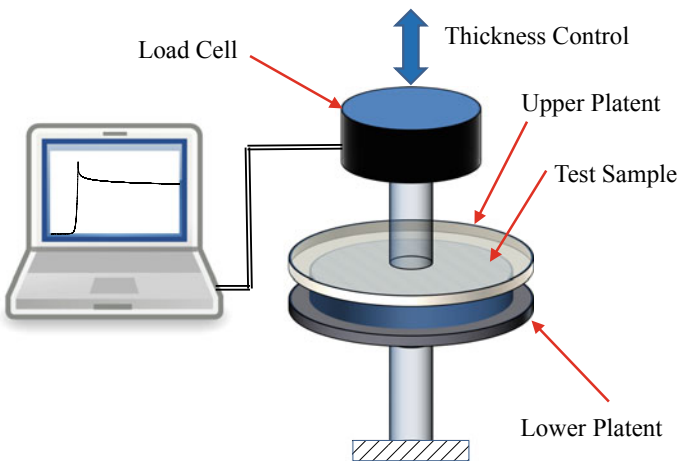


**Fig. 1.4** Illustration of experimental setup of reinforcement compaction characterization

### 1.4.1.3 Numerical Simulations

Numerical simulation using finite element method (FEM), is a powerful tool to predict the compaction behavior of fiber reinforcements. Compaction simulations are carried out by mimicking the loading conditions on a geometrical configuration. The main challenge is to obtain accurate models for the geometry of woven reinforcements while simultaneously being able to describe their mechanical and physical behavior. The prediction quality of an FEM analysis of a fibrous structure strongly depends on the model, i.e. its geometry, the material model, and the associated boundary, as well as contact conditions. The inhomogeneous structure of woven reinforcements and locally varying material properties associated with the fiber architecture make their modeling a complex and challenging task. It is necessary to consider realistic textile geometries in order to accurately predict the performance of 3D woven reinforcements and their composites. Importantly, 3D woven reinforcements feature a more complex architecture than 2D woven fabrics.

### 1.4.1.4 Micro CT Assisted Compaction

Micro CT has been used by a number of researchers to investigate the internal geometry changes due to compaction and other loading conditions typical of those encountered in LCM processes. Through special experimental procedures, Hemmer et al. [10] quantified the evolution of a given dual-scale fibrous microstructure under controlled infusion. Emerson et al. [11] quantified the fiber re-orientation during axial compression of a composite through time-lapse micro CT imaging and individual fiber tracking. Vanaerschot et al. [12] quantified geometrical variability of laminated composite textiles in terms of geometrical parameters of the tows such as, centroid location, aspect ratio, area, orientation, etc. using the micro CT images of a composite part produced by resin transfer molding. In a similar study by the same authors, a dry 3D reinforcement sample was used for acquiring the micro CT images [13]. Mahadik et al. [14] used five different potted samples at each fiber volume fraction to study the yarn waviness caused by compaction of two 3D angle interlock woven reinforcements. However, all of these studies presented geometrical data for a single  $V_f$  and the effects of compaction were not included. An in-house designed compression rig was used by Yousaf et al. [15, 16] to obtain micro CT images of an E-glass plain woven reinforcement under different compressive loadings to validate compaction simulation using digital element methods. The micro CT images were used to measure the geometrical features of the meso-structure.

## 1.4.2 Permeability Characterization

Similar to the compaction characterization, there are various approaches to permeability characterization as well. These are described below.